A new method for fabricating high density and large aperture ratio liquid microlens array

Hongwen Ren,[1,2] Daqiu Ren,[2] and Shin-Tson Wu[2]

[1]*Department of Polymer Nano-Science and Engineering, Chonbuk National University, Chonju, Chonbuk, 561-756, Republic of South Korea*
[2]*College of Optics and Photonics, University of Central Florida, Orlando, Florida 32816, USA*
swu@mail.ucf.edu

Abstract: Conventional liquid microlens arrays are facing bottlenecks in controlling droplet size and shape, and limited aperture ratio. We report a new liquid/solvent approach to overcome these obstacles for making uniform droplet array and achieving ~90% aperture ratio. The droplets are very stable due to the pinning effect of the polymer walls and substrate surfaces. Using the fabricated droplet array, we demonstrate a tunable-focus microlens array based on dielectrophoretic effect. The microlens array exhibits a large dynamic range and fast response time (tens of milliseconds). Besides liquid microlens arrays, this fabrication method also opens a new door for making other tunable photonic devices.

©2009 Optical Society of America

OCIS codes: (010.1080) adaptive optics; (220.3630) lens; (230.2090) electro-optical devices

References and links

1. B. Berge, and J. Peseux, "Variable focus lens controlled by an external voltage: an application of electrowetting," Eur. Phys. J. E **3**(2), 159–163 (2000).
2. L. Dong, A. K. Agarwal, D. J. Beebe, and H. Jiang, "Adaptive liquid microlenses activated by stimuli-responsive hydrogels," Nature **442**(7102), 551–554 (2006).
3. S. Grilli, L. Miccio, V. Vespini, A. Finizio, S. De Nicola, and P. Ferraro, "Liquid micro-lens array activated by selective electrowetting on lithium niobate substrates," Opt. Express **16**(11), 8084–8093 (2008).
4. T. Krupenkin, S. Yang, and P. Mach, "Tunable liquid microlens," Appl. Phys. Lett. **82**(3), 316–318 (2003).
5. S. Kuiper, and H. W. Hendriks, "Variable-focus liquid lens for miniature cameras," Appl. Phys. Lett. **85**(7), 1128–1130 (2004).
6. C. C. Cheng, C. A. Chang, and J. A. Yeh, "Variable focus dielectric liquid droplet lens," Opt. Express **14**(9), 4101–4106 (2006).
7. H. Ren, H. Xianyu, S. Xu, and S. T. Wu, "Adaptive dielectric liquid lens," Opt. Express **16**(19), 14954–14960 (2008).
8. H. Ren, and S. T. Wu, "Tunable-focus liquid microlens array using dielectrophoretic effect," Opt. Express **16**(4), 2646–2652 (2008).
9. S. Xu, Y. J. Lin, and S. T. Wu, "Dielectric liquid microlens with well-shaped electrode," Opt. Express **17**(13), 10499–10505 (2009).
10. C. A. Lopez, and A. H. Hirsa, "Fast focusing using a pinned-contact oscillating liquid lens," Nat. Photonics **2**(10), 610–613 (2008).
11. S. Xu, H. Ren, Y. J. Lin, M. G. J. Moharam, S. T. Wu, and N. Tabiryan, "Adaptive liquid lens actuated by photo-polymer," Opt. Express **17**(20), 17590–17595 (2009).
12. J. S. Patel, and K. Rastani, "Electrically controlled polarization-independent liquid-crystal Fresnel lens arrays," Opt. Lett. **16**(7), 532–534 (1991).
13. H. Ren, and S. T. Wu, "Adaptive liquid crystal lens with large focal length tunability," Opt. Express **14**(23), 11292–11298 (2006).
14. G. Li, P. Valley, M. S. Giridhar, D. L. Mathine, G. Meredith, J. N. Haddock, B. Kippelen, and N. Peyghambarian, "Large-aperture switchable thin diffractive lens with interleaved electrode patterns," Appl. Phys. Lett. **89**(14), 141120 (2006).
15. G. Beadie, M. L. Sandrock, M. J. Wiggins, R. S. Lepkowicz, J. S. Shirk, M. Ponting, Y. Yang, T. Kazmierczak, A. Hiltner, and E. Baer, "Tunable polymer lens," Opt. Express **16**(16), 11847–11857 (2008).
16. N. Chronis, G. L. Liu, K. H. Jeong, and L. P. Lee, "Tunable liquid-filled microlens array integrated with microfluidic network," Opt. Express **11**(19), 2370–2378 (2003).
17. D. Zhang, V. Lien, Y. Berdichevsky, J. Choi, and Y. H. Lo, "Fluidic adaptive lens with high focal length tunability," Appl. Phys. Lett. **82**(19), 3171–3172 (2003).
18. F. Schneider, J. Draheim, R. Kamberger, P. Waibel, and U. Wallrabe, "Optical characterization of adaptive fluidic silicone-membrane lenses," Opt. Express **17**(14), 11813–11821 (2009).

19. J. Chen, W. Wang, J. Fang, and K. Varahramyan, "Variable-focusing microlens with microfluidic chip," J. Micromech. Microeng. **14**(5), 675–680 (2004).
20. P. Penfield, and H. A. Haus, *Electrodynamics of Moving Media* (MIT, Cambridge, 1967).
21. H. Ren, S. T. Wu, and Y. H. Lin, "In situ observation of fringing-field-induced phase separation in a liquid-crystal-monomer mixture," Phys. Rev. Lett. **100**(11), 117801 (2008).

1. Introduction

Adaptive focus lenses based on liquid [1–11], liquid crystal [12–14], polymer [15], and elastic membrane [16–19] have been studied extensively attempting for applications in imaging, optoelectronic, and biometrical devices. Among them, liquid lenses are particularly attractive because the liquid surface tension produces a nearly perfect spherical shape. Two types of liquid lens have been developed: electrowetting lens [1,3–5] and dielectrophoresis lens [6–9]. These two lenses exhibit some similar features, e.g., two immiscible liquids are employed in the lens cell; one liquid forms droplets on the inner surface of bottom substrate and the other liquid fills the surrounding space of the droplets. In an electrowetting lens, one liquid is conductive and the contact angle of the droplet is controlled by an electrostatic force, which in turn changes the droplet shape. As for a dielectriophoretic (also called dielectric) lens, the two employed liquids are nonconductive and they have different dielectric constants. When the two liquids experience an inhomogeneous electric field, the generated dielectric force reshapes the droplet surface and changes the focal length of the lens. In conventional designs, it is easy to fabricate a single liquid lens based on these two approaches. However, it is quite challenging to disperse a liquid into droplet array. This is because several factors have to be considered simultaneously, e.g., the position of each droplet, droplet size, droplet shape, droplet uniformity, and aperture ratio of the whole array.

To overcome these obstacles, here we report a novel approach for fabricating liquid droplet array. Our approach includes three steps: 1) forming a cavity array, 2) filling the cavity with liquid and solvent, and 3) evaporating the solvent. Using this approach, various droplet arrays can be developed easily. To illustrate the fabrication procedures, we prepared a dielectrophoretic microlens array and characterized its imaging properties

2. Fabrication method

Liquid droplet plays a key role in a liquid lens. To form droplet array, we first prepared a cavity array. The processing sequence is illustrated in Fig. 1(a). First, we spread a UV curable monomer, such as NOA65 (Norland Optical Adhesive), on a thin glass substrate surface using a steel blade. After coating, the film is placed in horizontal direction for several minutes so that the thickness of the film becomes more uniform. The film thickness is controlled at ~20 μm. The film is then exposed to UV light through a photomask. We then use a solvent, such as ethanol, to rinse the cured film. When the unexposed monomer NOA65 is removed thoroughly, a solid polymeric cavity array is obtained. The geometry of the cavity can be controlled by the pattern of the photomask. In our experiment, we use two photomasks with square and circular patterns.

To make a droplet array, we chose a suitable liquid, such as oil (SL-5267, refractive index n=1.67) as the droplet material. The oil is clear and its refractive index n~1.67 and dielectric constant ε_1~5. Due to the large surface tension (~50 dynes/cm), it is impossible to form a droplet array by directly filling it into the tiny cavities. To solve this problem, we mixed the oil with a solvent. The solvent served for two purposes: it significantly decreased the surface tension of the oil, and it diluted the oil concentration in the mixture. When a small amount of the mixture was dripped on the patterned film surface, as Fig. 1(b) shows, the film was then heated in order to accelerate the solvent evaporation. After the solvent was evaporated thoroughly, the oil formed uniform droplets in the cavities, as shown in Fig. 1(c).
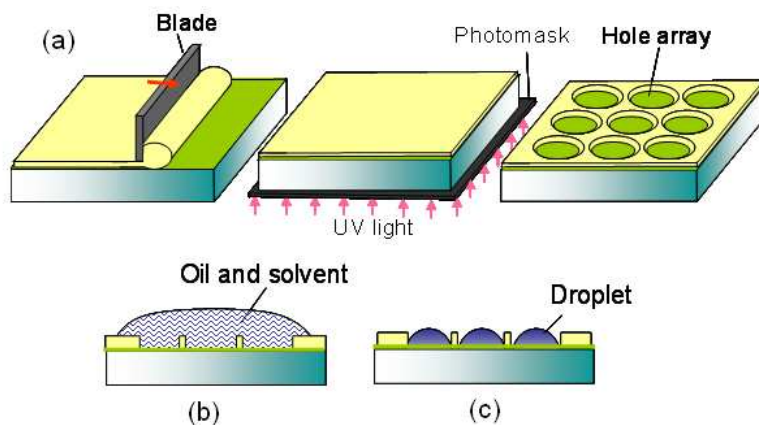
Fig.1. Procedure for fabricating a liquid droplet array: (a) Coating UV polymer on substrate surface (left). UV exposure through a photomask (middle) and forming a cavity array (right). (b) Dripping the oil mixture on the patterned cavity array film, and (c) Solvent evaporation.

3. Results and discussion

Based on these procedures, we prepared two samples with different droplet patterns: square and circular. We chose dichloromethane as the solvent to mix with the oil (concentration ~ 15 wt%). Figure 2(a) shows a droplet array observed under an optical microscope. Each droplet in the array has a square shape. The aperture of each droplet is ~60 μm and the adjacent droplets are separated by a 3-μm-thick polymer wall. The droplet has uniform size. Figure 2(b) shows the droplet array with circular aperture. The diameter of each droplet is ~50 μm and the distance between neighboring droplets is ~8.5 μm. Such a distance is dependent on the formed cavity pattern and it can be adjusted by the oil concentration in the mixture.
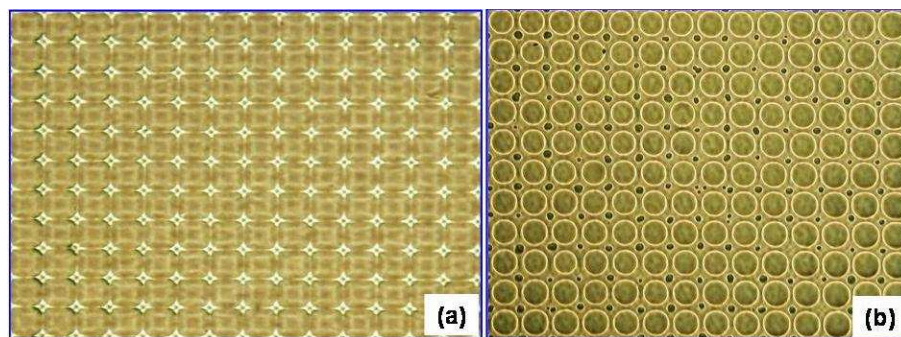

Fig. 2. The prepared liquid droplet arrays observed using an optical microscope: (a) Droplet with square aperture, and (b) Droplet with circular aperture.

To prove that the oil indeed forms droplets separately in the tiny cavities, we focused on the filled and empty cavities of sample 1 using an optical microscope. Results are shown in Fig. 3(a). The black squares in the bottom region are the empty cavities which look quite different from the oil-filled cavities. However, both empty and oil-filled cavities are clearly separated by a thin polymer wall. To observe the image performance of this droplet array, we typed a small letter "A" on a piece of transparency and placed such an object under the droplet array. By adjusting the distance between the droplet array and the object, a clear image was observed under white light illumination, as shown in Fig. 3(b). In contrast to the original object, the image "A" was inverted. The focal length of the droplet was measured to be

~240 µm. As for the empty cavities (bottom two rows), the displayed images were quite blurry.
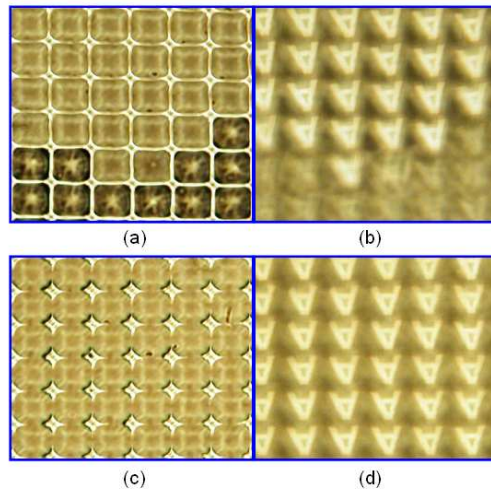

Fig. 3. Droplet arrays prepared under different conditions: (a) Oil-filled cavities vs. empty cavities (bottom two rows), (b) their imaging properties, (c) a droplet array with neighboring droplets connected, and (d) its imaging property.

To further confirm that the exposed polymer wall in Fig. 3(a) is indeed isolated from the adjacent oil droplets, we filled the left empty cavities of sample 1 with a larger amount of the mixture. After solvent evaporation the oil was remained in the cavities, but the polymer wall between the adjacent droplets could not be seen, as shown in Fig. 3(c). This result implies that the size of each droplet is increased and the adjacent droplets are connected to each other. Our results show that the size of each droplet in the array can be controlled by the amount of the mixture. Figure 3(d) shows the image array of the droplets. We find that the observed image is also clear although the adjacent droplets are not isolated. In this case, the focal length of the microlens was measured to be ~255 µm. Due to the action of oil surface tension the surface of each droplet still keeps the spherical or quasi-spherical shape.

The demonstrated droplet array can be used for preparing a microlens array. The droplets with circular aperture usually have a better image performance than the square ones due to geometric symmetry. Here we use the sample shown in Fig. 2(b) to prepare a dielectric microlens array. The basic lens cell structure is shown in Fig. 4(a). From top to bottom is: indium tin oxide (ITO) electrode (top glass plate is not shown), top liquid, droplet array, and bottom ITO electrode. Here we chose glycerol as the top liquid because glycerol and oil have several merits as lens materials: 1) they are immiscible, 2) glycerol has a large dielectric constant (ε~47) and low refractive index (n~1.47), and 3) their densities match very well (D~1.25 for glycerol and D~1.26 for the oil) so that the gravity effect is negligible when the lens cell is placed in vertical direction.

In our experiment, the thickness of the lens cell was controlled at ~125 µm. In the relaxed state, the droplet has a contact angle (θ) with the polymer wall surface, as Fig. 4(a) depicts. Since the droplet exhibits a lens behavior, its focal length (f) can be calculated from following equation [4]:

$$f^3 = \frac{3V_d}{\pi(1-\cos\theta)(2-\cos^2\theta-\cos\theta)(n_1-n_2)^3} , \qquad (1)$$

where V_d is the volume of the droplet, n_1 and n_2 the refractive index of the droplet and the top liquid, and θ the contact angle.
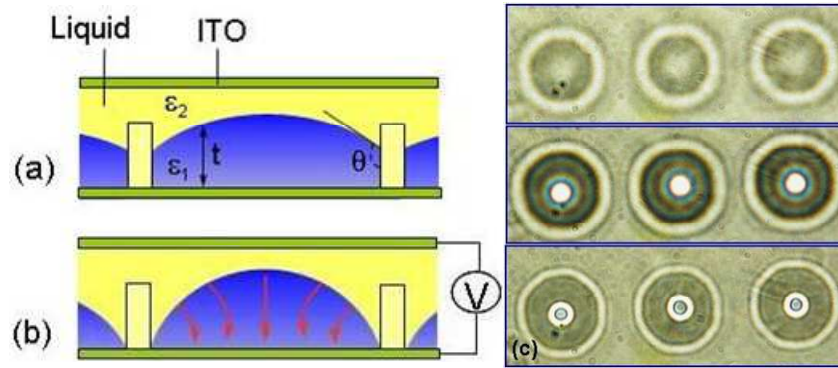
Fig. 4. Side-view structure of a microlens and the focus change of the lens versus voltage: (a) A relaxed state, (b) A contracting state, and (c) Imaging behaviors of the 1×3 microlens array at V=0 (top), V=120 V_{rms} (middle), and V=170 V_{rms} (bottom).

According to Kelvin theory, when an electric field is applied to the liquid droplet the droplet surface experiences a dielectric force (*F*) as [20,21]:

$$F = \frac{1}{2}\varepsilon_0(\varepsilon_2 - \varepsilon_1)\nabla(E \bullet E),\qquad(2)$$

where ε_0 represent the permittivity of free space and E denotes the electric field on the curved droplet surface. Due to the centrosymmetric inhomogeneous liquid droplet, the droplet border will bear a stronger force than that in the droplet center. When the dielectric force is strong enough, the contact angle and droplet shape are altered as depicted in Fig. 4(b), in which the red lines denote the electric field directions at different positions. As a result from Eq. (1), the focal length of the droplet is changed accordingly. When the applied voltage is high enough, the liquid interface may approach the corner of the cell walls, but there will be no abrupt profile change because the surface tension of the two liquids and the surface anchoring of the wall and substrate can balance the change smoothly. Thus, the surface of the droplet changes smoothly and the liquid lens exhibits high optical performances.

To observe the tunable focal length of the microlens array, we placed the lens cell on a microscope stage which can travel in vertical direction. Figure 4(c) shows the recorded images of a 1×3 lens array at V=0, 120, and 170 V_{rms} (300 Hz) from top to bottom, respectively. At V=0, we intentionally adjusted the position of the cell such that it was in a large defocused state. Thus, its border is highly circular with some rings inside the circle. At V=120 V_{rms}, we got highly focused spots at the center. At V=170 V_{rms}, the light in the center presents blue color and the intensity is relatively weak. Most of the light is focused on a circular zone around the center. Due to the small Abbe number of the employed oil (~22), color dispersion should be the main cause for the observed lens aberration.
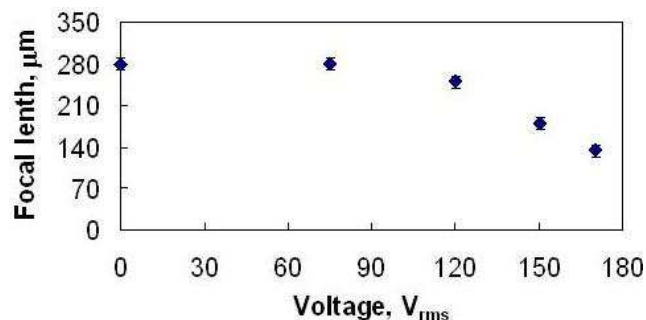

Fig. 5. The voltage-dependent focal length of a dielectric liquid lens.

To measure the focal length of the microlens, we first adjusted the position of the lens cell so that it focused on the droplet surface. Then we adjusted the cell position vertically until we saw a clear image. The distance the cell traveled is the focal length of the lens. The focal length of one microlens shown in Fig. 4(c) was measured at different voltages. Figure 5 depicts the measured voltage dependent focal length. At V=0, the focal length of the lens is $f\sim280$ μm. As the voltage increases, the focal length is decreased gradually. At V=170 V_{rms}, the focal length is decreased to ~135 μm.

Fast response time is desirable for an adaptive lens during focus change. To measure the switching speed of the lens, we used a collimated He-Ne laser beam to probe the cell at normal incidence. The transmitted beam was expanded by a glass lens and received by a photodiode detector. A diaphragm was placed right before the detector. At V=120 V_{rms}, we adjusted the diaphragm's aperture so that the focused beam passing through the diaphragm without any loss. When the voltage was turned off, the focal length of the microlens became longer. As a result, a portion of the laser beam was blocked by the diaphragm. Figure 6(a) shows the intensity change with time when a gated square-wave voltage burst (120 V_{rms}) was applied to the lens cell. The measured rise time is ~20 ms and decay time ~80 ms. The rise time is mainly dependent on the induced dielectric force, while the decay time is governed by the viscosity of the liquids and the related interfacial tensions.
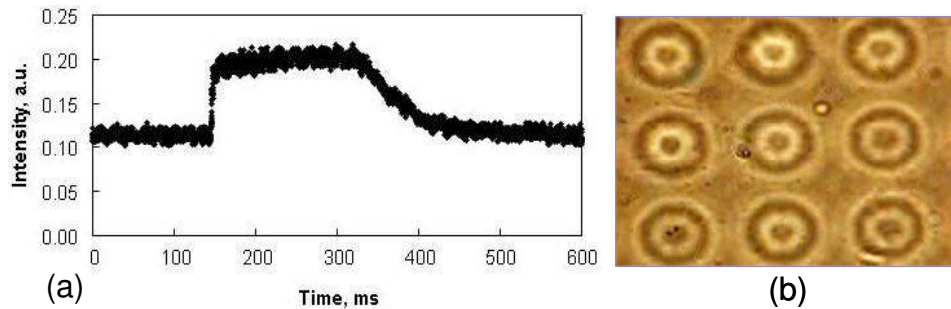

Fig. 6. (a) Measured response time of a microlens with circular aperture, and (b) dynamic tuning of 3×3 mircolens array driven from a defocused state to a focused state (Media 1).

To visually observe the dynamic tuning, we recorded a movie for tuning a 3x3 microlens array from a large defocused state to a focus state, as shown in Fig. 6(b). The response of all the microlenses is almost the same. The focal length tunability of each lens is wide and very uniform. In experiments, we measured the focal length with an ac voltage (300 Hz). In comparison to such a frequency, our lens response (~100 ms) is still too slow. Therefore, it will respond to the root-mean-square voltage, but not to the individual voltage pulse. As for our lens cell, the position of each droplet in the cavity is very stable once the solvent is evaporated thoroughly because the droplet is strongly pinned by the substrate surface and the surrounding polymer walls. Moreover, the chosen glycerol is insoluble with SL-5267 oil and their densities match well, the gravity effect is negligible when the lens cell is placed in vertical direction.

4. Conclusion

We have developed a method for fabricating liquid droplet array and dielectrophoretic microlens array. To prove principles, we demonstrated a uniform square droplet array and a circular droplet array. The adjacent droplets are separated by a 3-μm-thick polymer wall, so the aperture ratio reaches ~90% for the square-shaped polymer walls. These droplets are very stable due to the pinning effect of the polymer walls and substrate surfaces. As an adaptive-focus microlens, its focal length can be tuned in a wide range and its response time is ~80 ms. The described approach can be extended to making other tunable photonic devices, such as striped liquid grating, Fresnel zone lens, and liquid crystal droplet array for 2D grating.